Mem. S.A.It. Vol. 81, 998

Memorie della

The role of primary ^{16}O as a neutron poison in AGB stars and fluorine primary production at halo metallicities

R. Gallino[1,3], S. Bisterzo[1], S. Cristallo[2,3], and O. Straniero[3]

[1] Dipartimento di Fisica Generale, Università di Torino, 10125 (To) Italy
e-mail: gallino@ph.unito.it
[2] Departamento de Fisica Teorica y del Cosmos, Universidad de Granada, Campus de Fuentenueva, 18071 Granada, Spain
[3] INAF-Osservatorio Astronomico di Collurania, via M. Maggini, 64100 Teramo, Italy

Abstract. The discovery of a historical bug in the *s*-post-process AGB code obtained so far by the Torino group forced us to reconsider the role of primary ^{16}O in the ^{13}C-pocket, produced by the ^{13}C(α, n)^{16}O reaction, as important neutron poison for the build up of the *s*-elements at Halo metallicities. The effect is noticeable only for the highest ^{13}C-pocket efficiencies (cases ST*2 and ST). For Galactic disc metallicities, the bug effect is negligible. A comparative analysis of the neutron poison effect of other primary isotopes (^{12}C, ^{22}Ne and its progenies) is presented. The effect of proton captures, by ^{14}N(n, p)^{14}C, boosts a primary production of fluorine in halo AGB stars, with [F/Fe] comparable to [C/Fe], without affecting the *s*-elements production.

Key words. Stars: nucleosynthesis – Stars: C ans s rich – Stars: AGB

1. Introduction

We discovered an old bug in the *s*-post-process code that follows the *s*-process production in AGB stars (Gallino et al. 1998; Straniero et al. 2003). In the ^{13}C-pocket, where the major neutron source ^{13}C(α,n)^{16}O is activated, the poison effect of ^{16}O was overlooked. Despite its very low neutron capture cross section, during the first ^{13}C-pocket, the large primary ^{16}O abundance makes the product σN dominate over the other major light neutron poisons in reducing the neutrons available for the Fe seeds. This is shown in Table 1 for case ST (Gallino et al. 1988), AGB initial mass M = 1.5 $M_{\odot}$, [Fe/H] = −2.3. Note that the neutrons captured by the very abundant primary ^{12}C are almost fully recycled by ^{13}C(α,n)^{16}O. In the computations, the efficiency of the ^{13}C-pocket in the interpulse is kept unchanged at every thermal pulse (TP) (see Käppeler et al. 2010, and references therein). In advanced TPs, the progressive addition in the He intershell of primary ^{14}N [1] makes ^{22}Ne and its progenies to become

Send offprint requests to: R. Gallino

[1] by conversion if the H-burning shell of primary ^{12}C mixed with the envelope by previous third dredge up (TDU) episodes, followed by conversion

Table 1. Light neutron poisons in the first and in the last ^{13}C-pocket (case ST) for an AGB model of initial mass 1.5 $M_{\odot}$, metallicity [Fe/H] = −2.3.

	$<\sigma>$ (mbarn) 30 keV	1^{st} pocket Number fraction	1^{st} pocket σN	last pocket Number fraction	last pocket σN
^{12}C	0.0154	1.7×10^{-2}	2.6×10^{-4}	1.6×10^{-2}	2.5×10^{-4}
^{16}O	0.0380	1.8×10^{-3}	6.8×10^{-5}	9.6×10^{-4}	3.6×10^{-5}
^{22}Ne	0.059	3.6×10^{-6}	2.1×10^{-7}	7.7×10^{-4}	4.5×10^{-5}
^{25}Mg	6.4	8.4×10^{-8}	5.4×10^{-7}	5.5×10^{-6}	3.5×10^{-5}
^{56}Fe	11.7	1.1×10^{-7}	1.3×10^{-6}	6.6×10^{-8}	7.7×10^{-7}

primary isotopes and to largely overcome the poisoning effect of ^{16}O.

For high ^{13}C-pocket efficiencies, cases ST*2 to ST, and metallicities [Fe/H] < 2, there is a sensible decrease of the *s*-element production in the envelope at the end of the AGB phase. This is shown in Fig. 1 for [h*s*/Fe] by comparing in the bottom panel the updated results with respect to previous results (top panel) in which the ^{16}O produced by α capture on ^{13}C was not accounted for. For lower ^{13}C-pocket efficiencies or for Galactic disk metallicities the differences are negligible. The [l*s*/Fe] ratio changes in the same way, so that the *s*-process indicator [h*s*/l*s*] is only marginally affected, as is evident in Fig. 2 by comparing the results of the top and bottom panels. Some differences are shown in the second *s*-process indicator, [Pb/hs], as reported in Fig. 3 . As indicated in Fig. 4, a large spread of ^{13}C-pocket efficiencies at any given metallicity appears necessary to account for spectroscopic observations of *s*-process enhanced stars. Spectroscopic observations of carbon-rich and *s*-process enhanced metal-poor stars (CEMP-s) encompass the range of theoretical predictions between ST/2 and ST/50, averaging around case ST/4. For Galactic disk *s*-enriched stars the spectroscopic observations of different classes of *s*-rich stars encompass the range of theoretical predictions of [h*s*/l*s*] between ST*2 and ST/3, averaging around the ST case. Spectroscopic observations are discussed in the review by Käppeler et al.(2010).

to primary ^{22}Ne by double α capture in the early phase of the next TP.

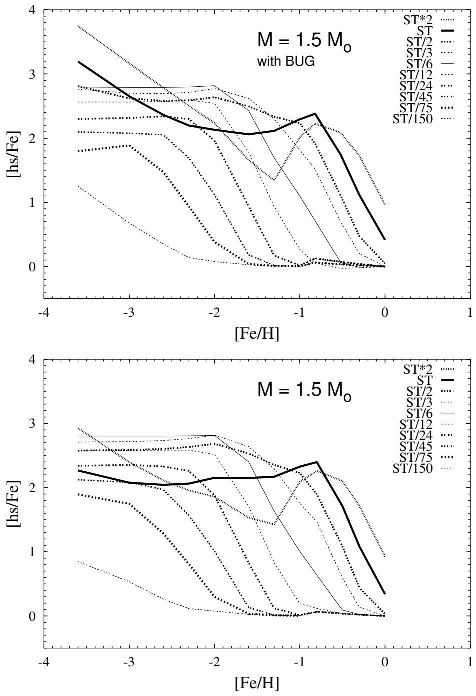

Fig. 1. The second *s*-peak [h*s*/Fe] for different ^{13}C-pocket efficiencies. Top panel: previous results with the ^{16}O bug in the pocket; bottom panel; updated results.

[Pb/hs] typically increases with decreasing metallicity.

2. Primary production of fluorine in low metallicity CEMP-s stars

Proton captures are now included in the post-process code to improve the prediction of fluo-

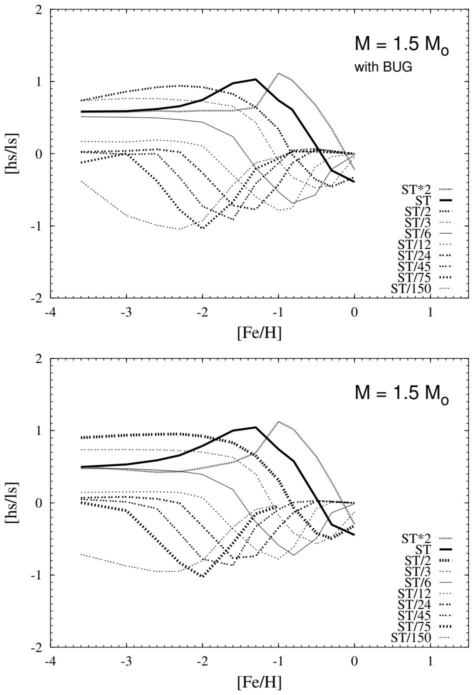

Fig. 2. The first *s*-process indicator [h*s*/l*s*] for different ^{13}C-pocket efficiencies. Top panel: previous results with the ^{16}O bug in the pocket; bottom panel: updated results.

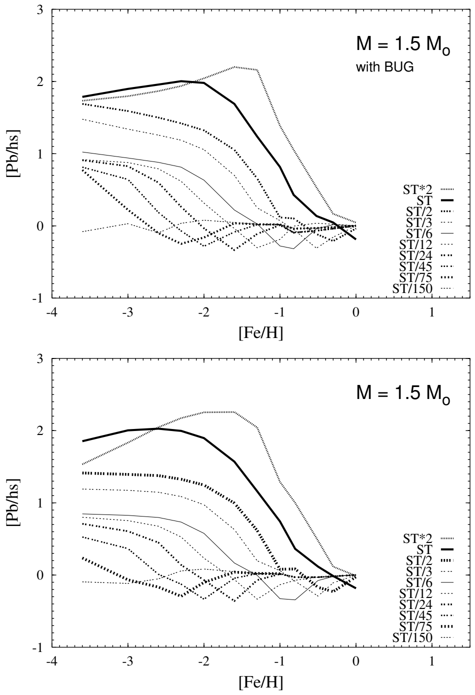

Fig. 3. The second *s*-process indicator [Pb/hs] for different ^{13}C-pocket efficiencies. Top panel: previous results with the ^{16}O bug in the pocket; bottom panel; updated results.

rine. Protons in the pocket and in the TP derive from $^{14}N(n, p)^{14}C$. Reaction rates of isotopes involving charged particles reactions involved in the various channels to ^{19}F are taken from the NACRE compilation (Angulo et al. 1999). Different channels to ^{19}F are:

- $^{18}O(n, \gamma)^{19}O(\beta^- \nu)^{19}F$
- $^{15}N(\alpha, \gamma)^{19}F$, where ^{15}N derives from $^{14}N(n, \gamma)^{15}N$ and $^{14}C(n, \gamma)^{15}C(\beta^- \nu)^{15}N$
- $^{18}O(p, \gamma)^{19}F$
- $^{18}O(p, \alpha)^{15}N(\alpha, \gamma)^{19}F$
- ^{13}C in the ashes of the H-burning shell: $^{13}C(\alpha, n)^{16}O$, $^{14}N(n, p)^{14}C$ and $^{18}O(p, \alpha)^{15}N$ in the early development of the TP, followed by $^{15}N(\alpha, \gamma)^{19}F$

For a recent discussion of the fluorine production in AGB stars we refer to Lugaro et al. (2004, 2008); Abia et al. (2009); Cristallo et al. (2009). Improvement of fluorine prediction, accounting for updated experimental measurements of reaction rates, will be discussed elsewhere. Table 2 shows the results of various tests to individuate the relative contribution to ^{19}F by different nuclear channels for an AGB model of 2 $M_{\odot}$, [Fe/H] = −2.3 and case ST/6. Actually, ^{19}F production does not depend much on the ^{13}C-pocket efficiency.

2.1. Fluorine in CEMP-s stars

Schuler et al. (2007), using the Phoenix spectrometer and Gemini-South telescope discovered a CEMP-s star, HE 1305+0132, with [Fe/H] = −2.5 ± 0.5 and very enhanced fluorine: [F/Fe] = 2.9. Subsequently, Schuler et al. (2008) with a higher resolution spectrum taken at the 9.2 m HET Telescope of the MacDonald Observatory, better estimated [Fe/H] = −1.9, and derived [C/Fe] = 1.7,

Table 2. Tests for the origin of fluorine.

Cases	[F/Fe]
No channels	0.00
Only $^{18}O(n, \gamma)^{19}O(\beta^- \nu)^{19}F$	1.18
Only $^{18}O(p, \gamma)^{19}F$	3.47
Only $^{18}O(p, \alpha)^{15}N$	3.50
Only $^{18}O(p, \alpha)^{15}N$ and No ^{13}C primary in the TP	2.16
All channels	3.80

Table 3. Fluorine and *s*-process productions for an AGB model of 2 $M_\odot$; [Fe/H] = –2.3; case ST/6.

Cases	[F/Fe]	[Y/Fe]	[La/Fe]	[Pb/Fe]
No protons	1.65	2.02	2.86	3.82
With protons	3.54	1.98	2.85	3.82
With protons + primary ^{13}C in the TP	3.80	2.01	2.86	3.81

Table 4. AGB model of 2 $M_\odot$; [Fe/H] = –2.3; *s*-process indexes for different ^{13}C-pocket efficiencies.

Cases	[l*s*/Fe]	[h*s*/Fe]	[Pb/Fe]	[h*s*/l*s*]	[Pb/h*s*]
ST × 2	1.68	2.13	4.21	0.45	2.08
ST	1.36	1.84	4.12	0.48	2.28
ST/3	1.55	2.50	4.00	0.95	1.50
ST/6	2.09	2.82	3.81	0.73	0.99
ST/12	2.41	2.85	3.42	0.44	0.57
ST/24	2.43	2.58	2.65	0.15	0.07
ST/45	2.20	1.83	1.72	-0.37	-0.11
ST/75	1.74	1.07	0.62	-0.67	-0.45
ST/150	0.97	0.14	0.13	-0.83	-0.01

[N/Fe] = 1.5, [Ba/Fe] = 0.9. The star is a giant of $T_{\rm eff}$ = 4462 ± 100 K; log g = 0.80 ± 0.30. Because of the First Dredge Up (FDU), the C-rich and *s*-process-rich material transferred by the winds of the primary AGB was diluted by 1 dex or more over the convective envelope of the observed star. Our typical AGB predictions would fit these data once 1 dex dilution is applied, with a further prediction of [Pb/Fe] ~ 2.5. However, a higher spectroscopic resolution is necessary for a definite confirmation and for detection of other heavy neutron-capture elements besides Ba.

3. Primary light elements production.

Together with carbon and fluorine, a number of light elements are synthesised in a primary

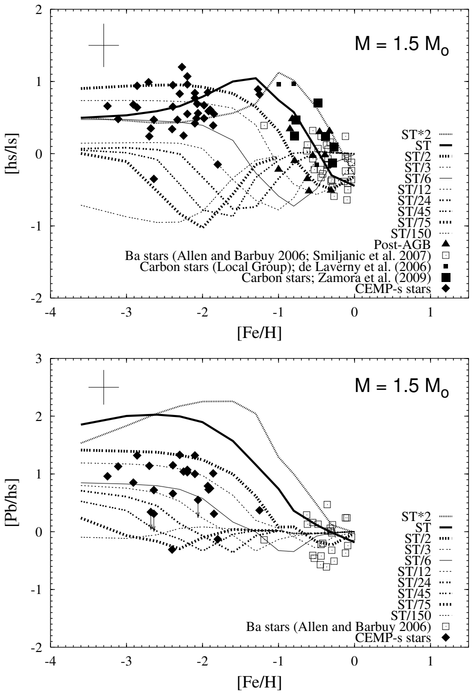

Fig. 4. Top panel. The first *s*-process indicator [h*s*/l*s*] for different ^{13}C-pocket efficiencies. Comparison between theoretical models and spectroscopic observations. References are: Galactic Post-AGB (filled triangles; Reddy et al. 2002, Van Winckel & Reyniers 2000, Reyniers et al. 2004, 2007); barium dwarfs and giants (open squares; Allen & Barbuy 2006; Smiljanic et al. 2007); metal-poor C(N) stars in the Local Group (small filled squares; de Laverny et al. 2006; Galactic C(N) stars (filled squares; Zamora et al. 2009). For CEMP-s stars (filled diamonds) references are Aoki et al. (2002, 2007); Barklem et al. (2005); Cohen et al. (2006); Goswami et al. (2006); Masseron et al. (2006); Pereira & Drake (2009); Preston & Sneden (2001); Roederer et al. (2008); Thompson et al. (2008); Van Eck et al. (2003).

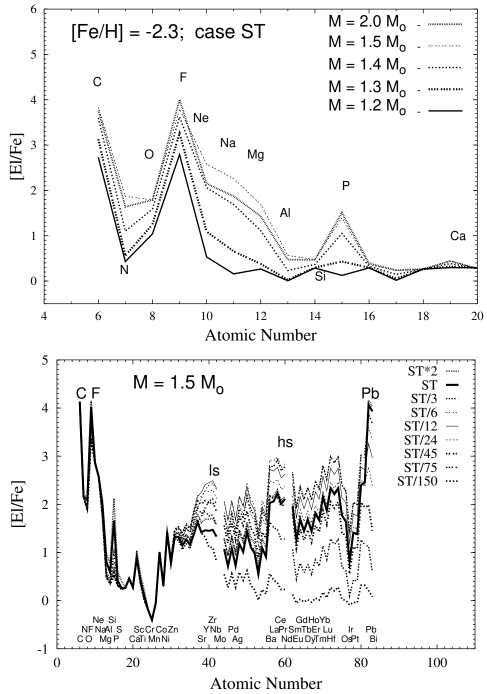

Fig. 5. (Top panel). Primary light elements expectation at [Fe/H] = −2.6, case ST and different AGB initial masses. (Bottom panel). [El/Fe] expectations as a function of the atomic number for AGB models of initial mass M = 1.5 $M_{\odot}$, metallicity [Fe/H] = −2.6, and different ^{13}C-pocket efficiencies.

way in low mass AGB stars of Halo metallicity. This includes Ne (in the form of ^{22}Ne) and its neutron capture progenies ^{23}Na. Besides, a very large overabundance of the ^{25}Mg and ^{26}Mg isotopes are obtained, by partial depletion of ^{22}Ne by α captures in the convective TP. Some primary ^{16}O is also produced by α captures on ^{12}C during the TP. Fig. 5 (top panel) shows the envelope AGB predictions at the last TDU episode of light elements for AGB models of metallicity [Fe/H] = −2.3, case ST and initial masses 2.0, 1.5. 1.4, 1.3 and 1.2 $M_{\odot}$. The general increase of the production factors with the increase of the initial mass is a direct consequence of the increase of the cumulative He-instershell mass mixed with the envelope, which grows with the number of TDU episodes. The primary contribution to nitrogen in the envelope was made in the inactivated H-shell that is also mixed with the envelope at each TDU episode. When comparing the C/N ratio observed in CEMP-s stars, one should consider that an important fraction of ^{12}C is possibly converted to ^{14}N by extra-mixing episodes in the observed star. The effect on the *s*-process by neutron capture of primary ^{16}O and ^{22}Ne is illustrated in Figure 6.

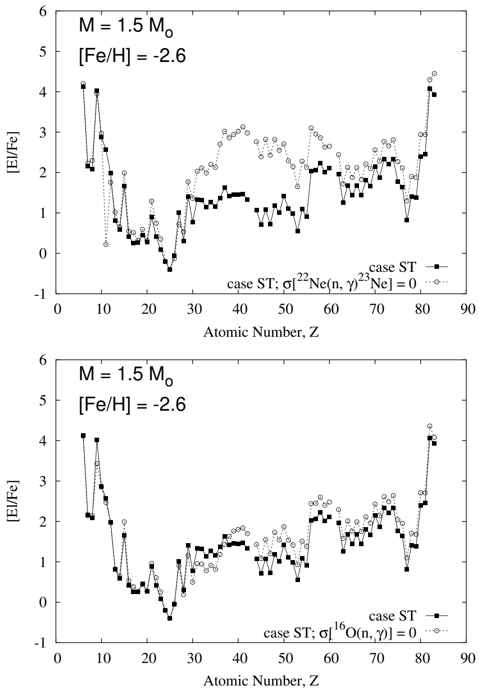

Fig. 6. The neutron poisoning effect of primary ^{22}Ne (top panel) and of primary ^{16}O (bottom panel) for an AGB model of [Fe/H] = −2.6, initial mass $M = 1.5\ M_\odot$ and case ST.

4. Conclusions

For Halo metallicities, the ^{16}O bug we had in the ^{13}C-pocket, which consisted in discarding neutron capture on the ^{16}O isotopes released by $^{13}C(\alpha, n)^{16}O$, affects [l*s*/Fe], [h*s*/Fe], [Pb/Fe] in an important way for the highest choices of the ^{13}C-pocket efficiency (cases ST × 2 and ST). Instead, the *s*-process indexes [h*s*/l*s*], [Pb/hs] are only marginally affected. For Galactic disc AGBs, the bug effect is negligible for all ^{13}C-pocket choices. Introduction of proton captures in the code does not affect the *s*-process abundances. However, it boosts the prediction of fluorine in very metal-poor *s*-enhanced stars. A primary production of F, comparable with the C enhancement, is predicted in AGB stars of low metallicity. The only spectroscopic observation of fluorine in a CEMP-s star, is the giant HE 1305+0132 by Schuler et al. (2007, 2008) and is quite in agreement with our F prediction. Higher resolution spectra are however necessary for a definite confirmation.

Acknowledgements. We are indebted to Franz Käppeler for his continuous support in implementing the experimental neutron capture measurements. R.G. deeply acknowledges for local support the Centre for Stellar and Planetary Astrophysics, School of Mathematical Sciences of the Monash University (Victoria, Australia) and the Organisers of the Workshop for a marvellous permanence at the University of Canterbury, Christchurch (New Zealand).

References

Abia, C., et al. 2009, ApJ, 694, 971
Allen, D., & Barbuy, B. 2006, A&A, 454, 917
Aoki, W., et al. 2002, ApJ, 580, 1149
Angulo, C., et al. 1999, Nucl. Phys. A 656, 3
Aoki, W., et al. 2007, ApJ, 655, 492
Barklem, P. S., et al. 2005, A&A, 439, 129
Bisterzo, S., et al. 2010, MNRAS, in press
Cohen, J. G., et al. 2006, AJ, 132, 137
Cristallo, S., et al. 2009, ApJ, 696, 797
de Laverny, P., et al. 2006, A&A, 446, 1107
Gallino, R., et al. 1998, ApJ, 497, 388
Goswami, A., et al. 2006, MNRAS, 372, 343
Käppeler, F., et al. 2010, Rev. Mod. Phys., accepted
Lugaro, M., et al. 2004, ApJ, 615, 934
Lugaro, M., et al. 2008, A&A, 484, L27
Masseron, T., et al. 2006, A&A, 455, 1059
Pereira, C. B., & Drake, N. A. 2009, A&A, 496, 791
Preston, G. W., & Sneden, C. 2001, AJ, 122, 1545
Reddy, B. E., et al. 2002, ApJ, 564, 482
Reyniers, M., et al. 2004, A&A, 417, 269
Reyniers, M., et al. 2007, A&A, 461, 641
Roederer, I. U., et al. 2008, ApJ, 679, 1549
Schuler, S. C., et al. 2007, ApJ, 667, L81
Schuler, S. C., et al. 2008, in NiC X, 2008, POS076
Smiljanic, R., G., et al. 2007, A&A, 468, 679
Straniero, O., et al. 2003, PASA, 20, 389
Thompson, I. B., et al. 2008, ApJ, 677, 556
Van Eck, S., et al. 2003, A&A, 404, 291
Van Winckel, H. & Reyniers, M., 2000, A&A, 354, 135
Zamora, O., et al. 2009, A&A, 508, 909